ARTICLE 4

FELIZ II THE PRUDENT: PROBABILITY RADIAL CLOSURE WITH HIGH ORDER VARIABLE C_F

Javier Silvestre
eeatom.blogspot com

ABSTRACT

Electronic extreme Probability (P_i) as orbital turn time [3] is obtained with its orbital circumference (c_i) [2] divided by its velocity (v_i) [1]. Regardless of PEP, whether 1 for 1s Hydrogen or 2 for rest, is verified that First Feliz Solution and its variable C_F with first-order approximation changes monotonous P_A increase when r_A increases [3].

Probability radial closure objective is achieved by using Second Feliz Solution with high order variable C_F (Theoretically to order infinite). Second Feliz Solution factors importance is studied and its relationship with d, division in which electronic extreme is found, is checked. As consequence, variable C_F behaviour differs to division near 1, intermediate and high.

KEYWORDS

Infinite order C_F, Second Feliz Solution, Electronic Extreme Probability, Probability radial closure, Victoria Equation.

INTRODUCTION

This is 4th article of 24 dedicated to atomic model based on Victoria equation (Articles index is at end). Similarity with orbital concept and electronic density is achieved with order-1 C_F that is included in orbital circumference (c_i) calculation [3]. Pythagorean triangle sides are: c_i [2], circular orbital height (H_i) [2] and radial distance (r_i) [1]. Three sides are created by division in which electronic extremes are found [1-3]. A extern electronic extreme (EE_A) is indicated with a suffix (r_A, H_A or c_A), B intern with b suffix (r_B, h_B or c_B) and i suffix is used to both electronic extremes (EE_i). All abbreviations are compiled, in conjunction with those included in [1], [2] and [3], at article end.

A electronic extreme Probability (P_A) closure is almost reached with First Feliz Solution and its order-1 C_F. However, probability observed is not cancelled at high radial distance ($r_A \approx 5.5$ A) that is provided by minimum division ($d_A=1$) (**Figure 1**). P_i non-cancellation is best observed in P_A. Figure 1 is made with Carbon outermost electron data used in [3]:

> Victoria Equation E_o is Carbon outermost electron ionization energy (IE) [4].
> PEP is equal to 2 according to P025.
> As in [3], 1 and 70 are used for z and MON respectively.

In addition, this fact of no enclosing A electronic extreme is maintained at greater radial distance as is $r_A \approx 52$ A (hypothetical d=0.2) (**Figure 2**), implying not insignificant P_A at high distances to nucleus. Therefore, although First Feliz Solution and its variable C_F

with first-order approximation has been an advance with respect constant C_F, complete probability enclosure must be achieved with Second Feliz Solution.

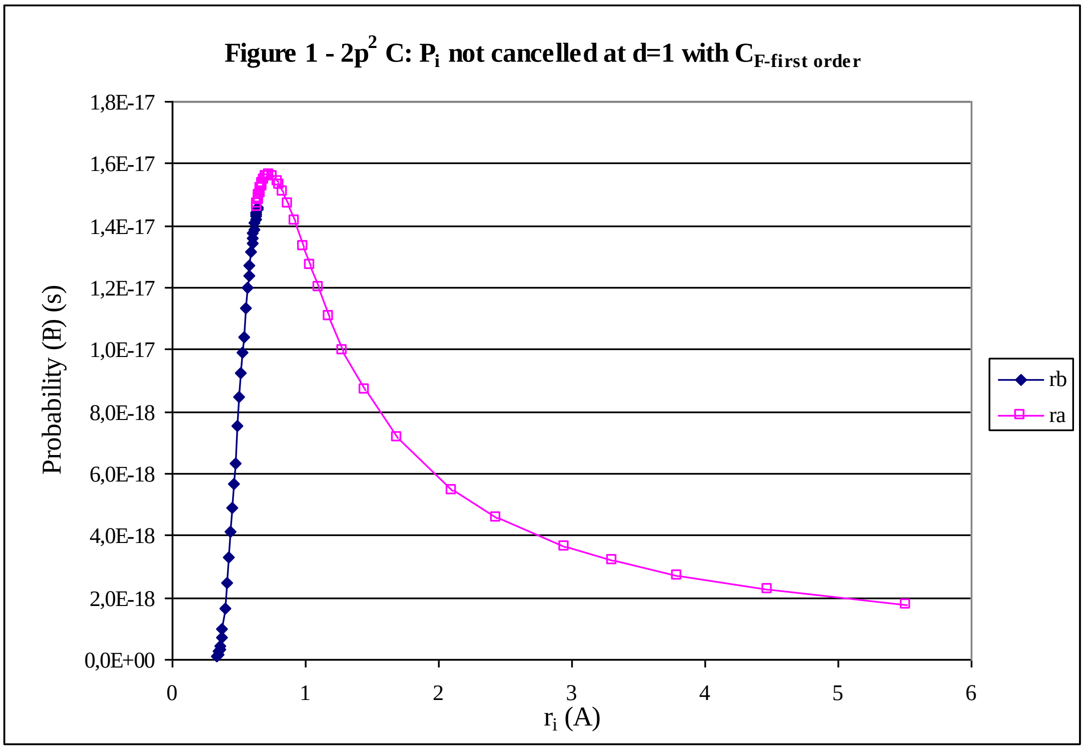

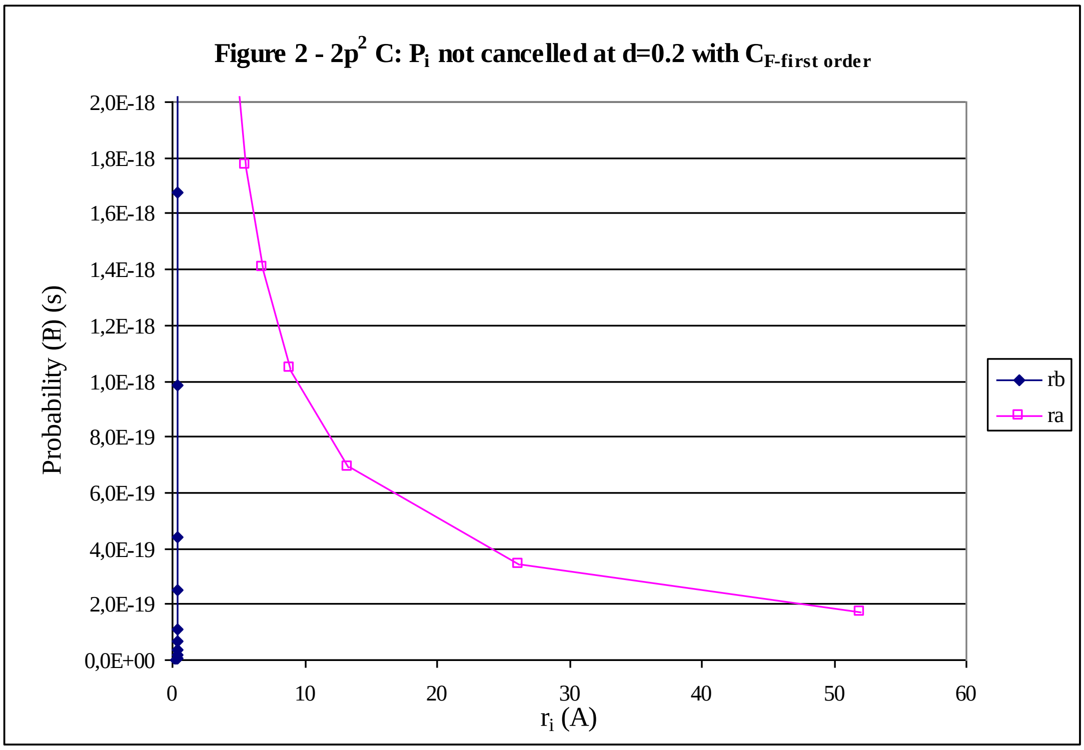

P29 Second Feliz Solution: Feliz II The Prudent. High-order Variable C_F

As introduced in P25 Feliz First Solution [3], Variable C_F with first-order approximation (1) is determined by division (d) in which electronic extremes is found and by two factors: PEP (P) and MON (M). Order-1 C_F variability is provided by wavelength division (d) since P and M are constants for a given electronic lobe.

$$(1)\ C_{F-\mathrm{FirstOrder}} = 2 + \frac{P*M}{d^P}$$

Total enclosure for A electronic extreme low division (d≈[1-2]) is achieved with Second Feliz Solution. This objective is reached by orbital circumference (c_i) compaction at low d (2). c_i is compressed with Order-J C_F and in which x goes from 1 to J. If J=1, implies that x can only be equal to 1 and consequently, (2) is transformed into (1). x is positive integer.

$$(2)\ C_{F-J\,\mathrm{order}} = 2 + \sum_{x=1}^{J} \frac{x^2 * P * M}{d^{x*P}}$$

Although (3) indicates that infinite J can be reached, is sufficient to work with order-10 CF, i.e. J=10, to simulate infinite J.

$$(3)\ C_{F-\mathrm{Infinite\,order}} = 2 + \sum_{x=1}^{\infty} \frac{x^2 * P * M}{d^{x*P}}$$

(4) is P_i function of r_i and d obtained in [3] with included Infinite-order C_F.

$$(4)\ P_i = \frac{\hbar}{2f\left(2 + \sum_{x=1}^{\infty} \frac{x^2 * P * M}{d^{x*P}}\right)} \frac{r_i}{z}$$

As example, 3-order Variable C_F is given by (5):

$$(5)\ C_{F-\mathrm{Third\,order}} = 2 + \frac{P*M}{d^P} + \frac{4*P*M}{d^{2P}} + \frac{9*P*M}{d^{3P}}$$

Table 1 shows how C_F varies as J increases. J ranges from 1 to 5 and then jumps to 10. J gain only influences when d is low and approaches 1. Even at low d as d=2, C_F increase is practically null when J is enhanced and goes from J=5 to J=10.

Table 1 - Impact of J increase on C_F

d	C_F 1	C_F 2	C_F 3	C_F 4	C_F 5	C_F 10
1	142,00	702,00	1962,00	4202,00	7702,00	53902,00
1,1	117,70	500,19	1211,43	2256,40	3605,81	13088,72
1,2	99,22	369,28	791,26	1312,21	1877,48	4252,80
1,3	84,84	280,91	541,95	816,55	1070,44	1770,15
1,4	73,43	219,20	386,54	538,33	659,33	894,40
1,6	56,69	142,14	217,24	269,39	301,22	337,07
1,8	45,21	98,56	135,60	155,93	165,73	173,05
2	37,00	72,00	91,69	100,44	103,86	105,70

2,5	24,40	38,74	43,90	45,36	45,73	45,84
3	17,56	24,47	26,20	26,54	26,60	26,61
4	10,75	12,94	13,25	13,28	13,28	13,28
5	7,60	8,50	8,58	8,58	8,58	8,58
6	5,89	6,32	6,35	6,35	6,35	6,35
7	4,86	5,09	5,10	5,10	5,10	5,10
8	4,19	4,32	4,33	4,33	4,33	4,33
10	3,40	3,46	3,46	3,46	3,46	3,46
12	2,9722	2,9992	2,9997	2,9997	2,9997	2,9997
14	2,7143	2,7289	2,7290	2,7290	2,7290	2,7290
16	2,5469	2,5554	2,5555	2,5555	2,5555	2,5555
20	2,3500	2,3535	2,3535	2,3535	2,3535	2,3535
30	2,1556	2,1562	2,1562	2,1562	2,1562	2,1562
40	2,0875	2,0877	2,0877	2,0877	2,0877	2,0877
50	2,0560	2,0561	2,0561	2,0561	2,0561	2,0561
60	2,0389	2,0389	2,0389	2,0389	2,0389	2,0389
70	2,0286	2,0286	2,0286	2,0286	2,0286	2,0286
80	2,0219	2,0219	2,0219	2,0219	2,0219	2,0219
90	2,0173	2,0173	2,0173	2,0173	2,0173	2,0173
100	2,0140	2,0140	2,0140	2,0140	2,0140	2,0140
150	2,0062	2,0062	2,0062	2,0062	2,0062	2,0062
200	2,0035	2,0035	2,0035	2,0035	2,0035	2,0035
250	2,0022	2,0022	2,0022	2,0022	2,0022	2,0022
300	2,0016	2,0016	2,0016	2,0016	2,0016	2,0016
350	2,0011	2,0011	2,0011	2,0011	2,0011	2,0011
800	2,0002	2,0002	2,0002	2,0002	2,0002	2,0002
1E+13	2,0000	2,0000	2,0000	2,0000	2,0000	2,0000

Three C_F zones are defined by (3) and corroborated with Table 1 and **Figure 3**. Figure 3 is C_F logarithmic representation as function of division logarithm. C_F logarithmic representation is performed for better visualization of the entire C_F range (C_F in Table 1 is from PEP to over $5.4 \cdot 10^4$).

1) Division $\rightarrow \infty$

The various summands (3) from x=1 to x=J are nullified because division is in denominator. Therefore, regardless of J order, (3) always tends to be equal to PEP when $d \rightarrow \infty$ (6). This fact is verified in Table 1 and also in Figure 3 where all curves tend asymptotically to: Log(PEP) = Log(2) ≈ 0,30103. Approximately, zone 1 is found in Log(division) > 1.

$$(6)\ (C_{F\ -\ Any\,Order})_{d\ \rightarrow\ \infty} = 2$$

2) Intermediate division

Greater x factors (3) increase in importance as division approaches 1. Equally roughly, zone 2 is located in range: 0 < Log(d) < 1. Since there is no single factor, curves separation according to their greater or less J is observed in Figure 3. Separation between curves becomes more evident as division decreases because high x factor importance grows.

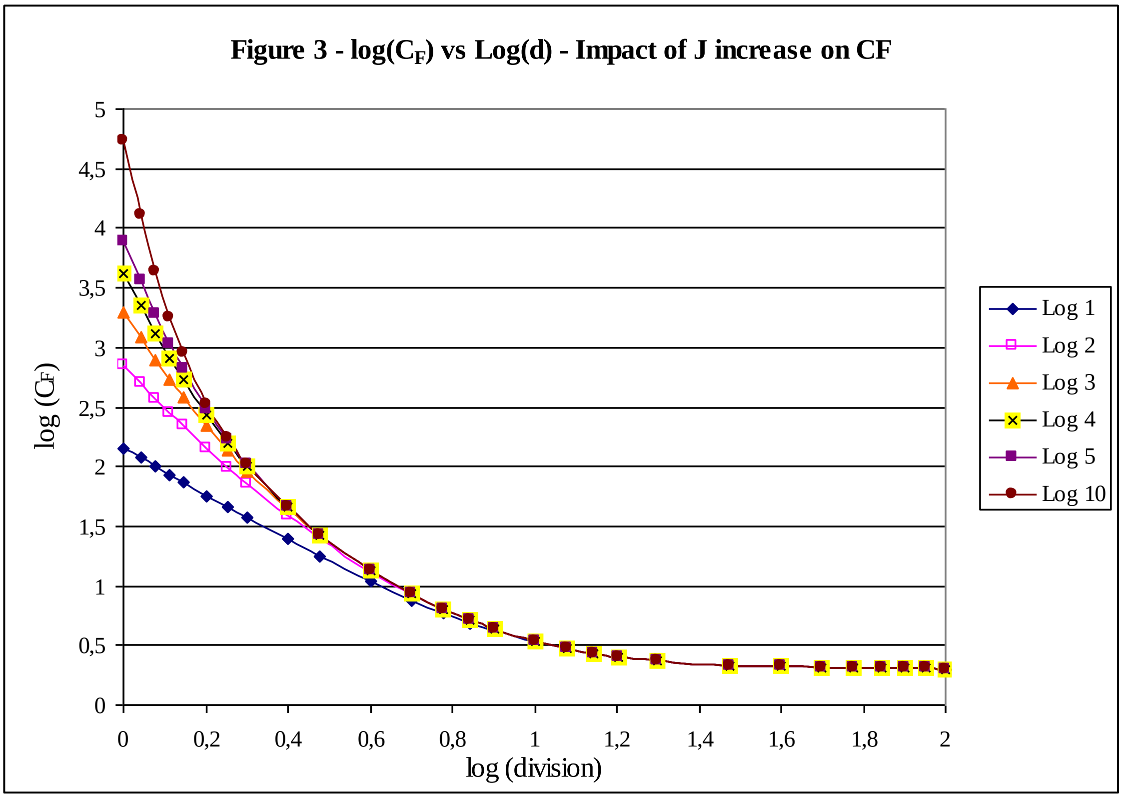

3) Division = 1 - Second Feliz Solution Division Limit

If d=1, (3) is simplified (7). As (7) has no variable terms, can be transformed into (8) which tends to infinite C_F. Si $C_F \to \infty$, then ci→0, and consequently Pi→0 (10) (where (9) is EE Probability definition seen in [3]). Consequently, minimum division is 1 because already has zero probability. In terms of Infinite-order C_F application, and although mathematically Victoria Equation can be solved for d>0, d must be greater that 1 to make probabilistic sense.

$$(7)\ (C_{F-\text{Infinite order}})_{d=1} = 2 + \sum_{x=1}^{\infty} x^2 * P * M$$

$$(8)\ (C_{F-\text{Infinite order}})_{d=1} = 2 + \infty^2 * P * M = \infty$$

$$(9)\ \text{EE Probabilit y} = P_i = \frac{c_i}{v_i} = \frac{\lambda_i}{2\pi\, C_F v_i}$$

$$(10)\ P_i(d=1) = \frac{\lambda_i}{2\pi v_i}\frac{1}{\infty} = 0$$

Radial distance (r_i) in X axis and Probability (P_i) with first-order C_F in Y axis are represented in Figure 1 and 2. In these figures, probability opening maintenance at high r_A is shown. First-order C_F and C_F with higher J order are included in **Figure 4**. Figure 4 radial distance is limited to 6 A in order to include division 1 with $(r_A)_{d=1}$=5,508099A. Nomenclature used is C_F (Compaction Factor) followed by number (J order), and letter A or B (electronic extreme). Selected J order is 1, 2, 3, 5 and 10.

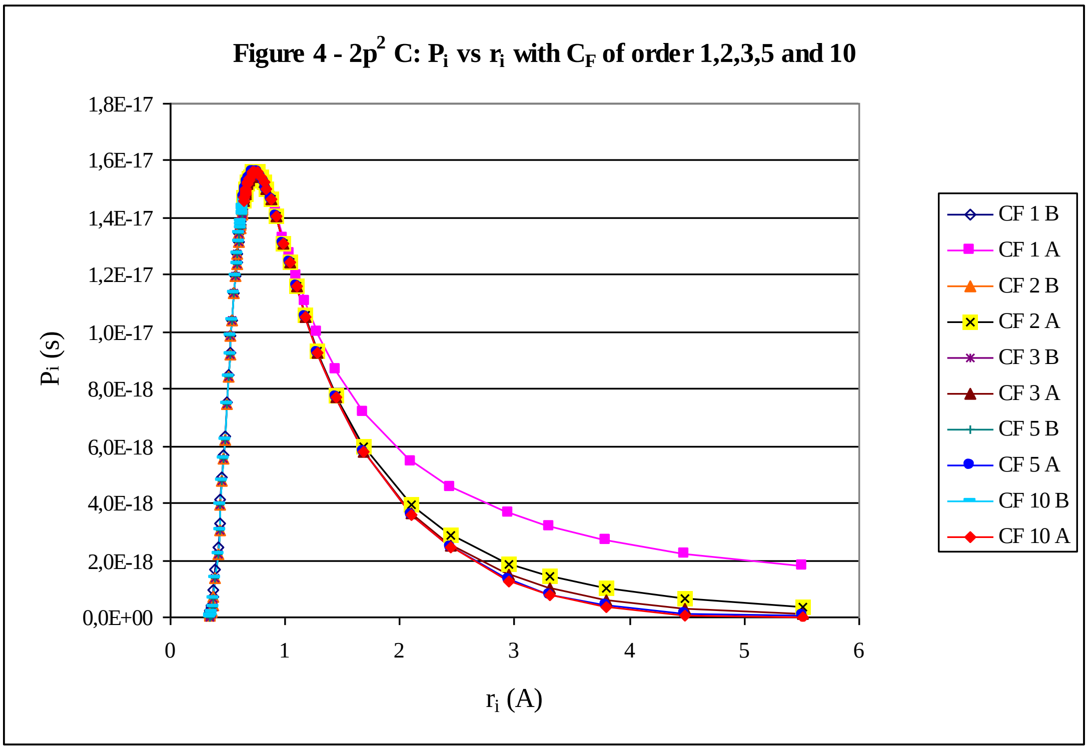

Difference, which between 1-order and 2-order C_F is clearly visible, declines markedly as J is increased. In fact, change between J=5 and J=10 is not nearly appreciable in Figure 4. To be able to observe it, Figure 4 zoom has been done in low d_A zone (**Figure 5**) which is the zone where the most noticeable effects of J changes are. In addition, low d_A zone should decrease its probability to meet Second Feliz Solution. B intern electronic extreme (EE_B) also modifies its P_B by increasing J. EE_B does not have the problem of extending probability to infinite as r_A can do. In addition, P_B is much lower when d_B is small and makes appear to be zero when d=1 for any J (Figure 4). P_i scale has been reduced by 30 with regard to Figure 5 (zoom for low d_A) to be able to observe reductions produced by J increase in low d_B zone (**Figure 6**).

Figure 5 - $2p^2$ C: P_i vs r_i with C_F of order 1,2,3,5 and 10 - Zoom for low d_A

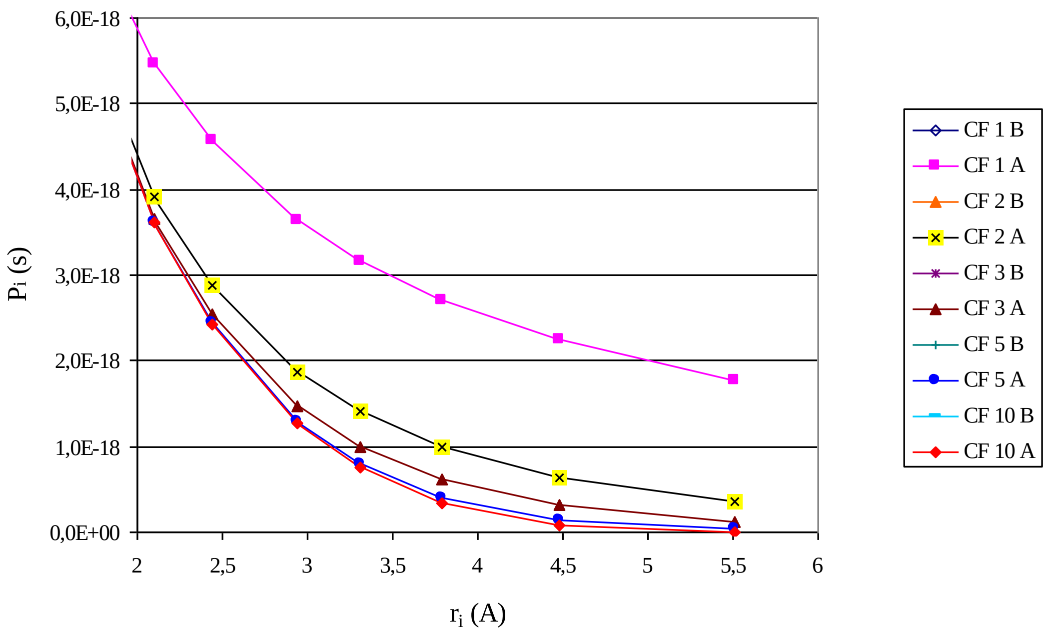

Figure 6 - $2p^2$ C: P_i vs r_i with C_F of order 1,2,3,5 and 10 - Zoom for low d_B

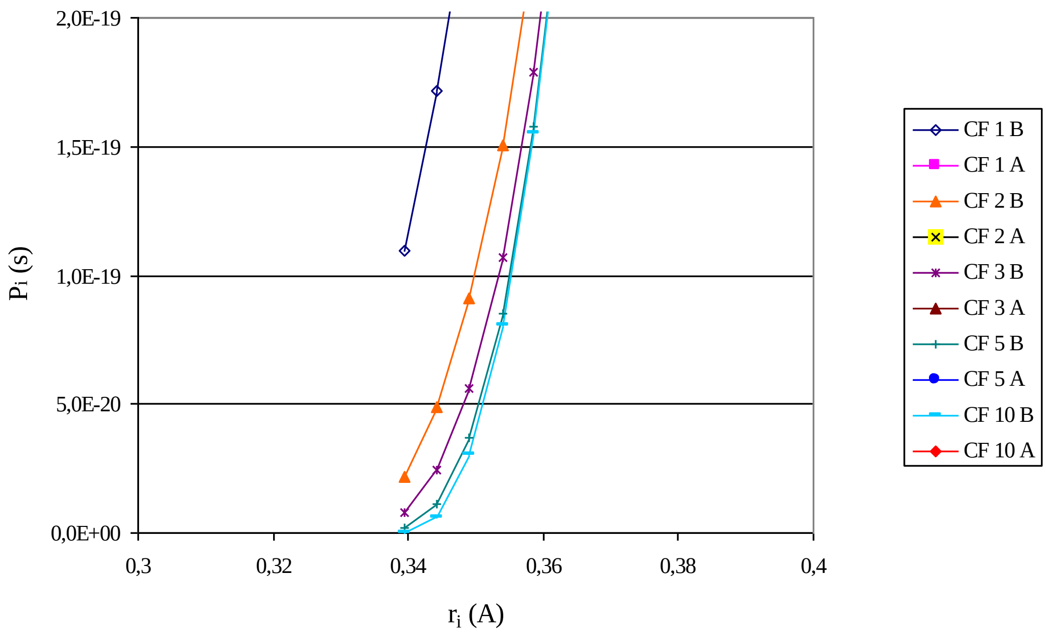

Maximum Probability area is expanded in **Figure 7**. In this figure, division with minor r_A represented is d_A=33. Each new point is one division unit plus. J change has little effect because maximum P_i is located in high division (d_A≈30). C_F is 2.1555 if J=1 and 2.1562 for J>1. For this reason, J=1 curve has slightly higher probabilities and its maximum is softly displaced. These effects are more pronounced if maximum P_i is located at low division because difference in C_F is higher as J increases (Table 1). $2p^2$ Maximum Probability is not exactly equal to [5] and [6] because MON and z are approximate until "Birth by probability coupling", introduced in [3], is exposed in later articles. Even so, difference between Figure 7 (≈74 pm) versus [5] and [6] (65 pm) is low.

Figure 7 - $2p^2$ C: P_i vs r_i with C_F of order 1,2,3,5 and 10 - Maximum Pi

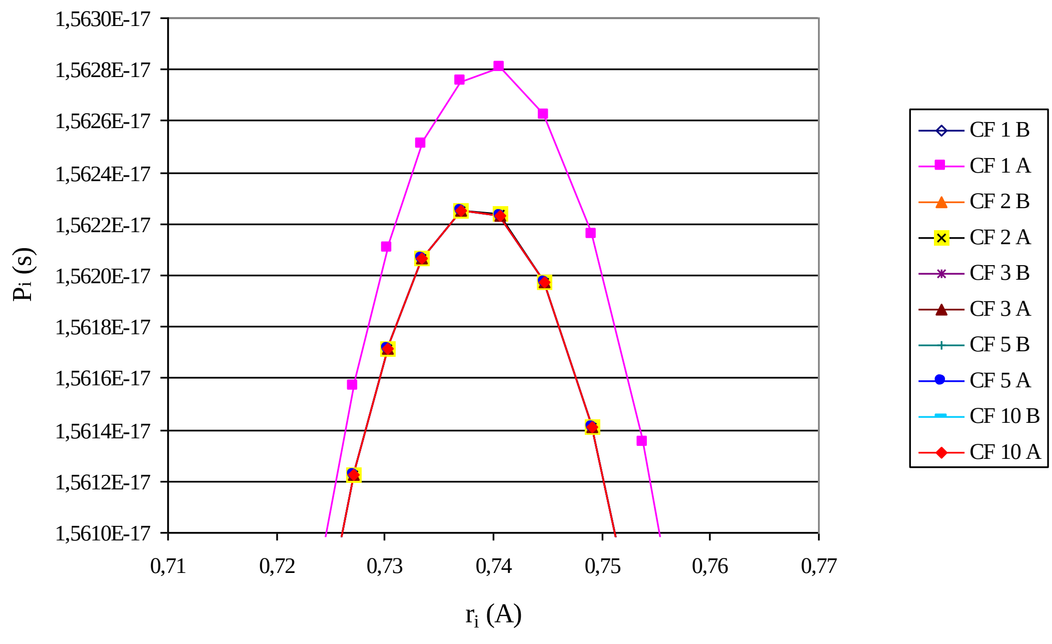

Figure 8 - $2p^2$ C: P_i vs r_i with PEP=2 z=1 and different MON

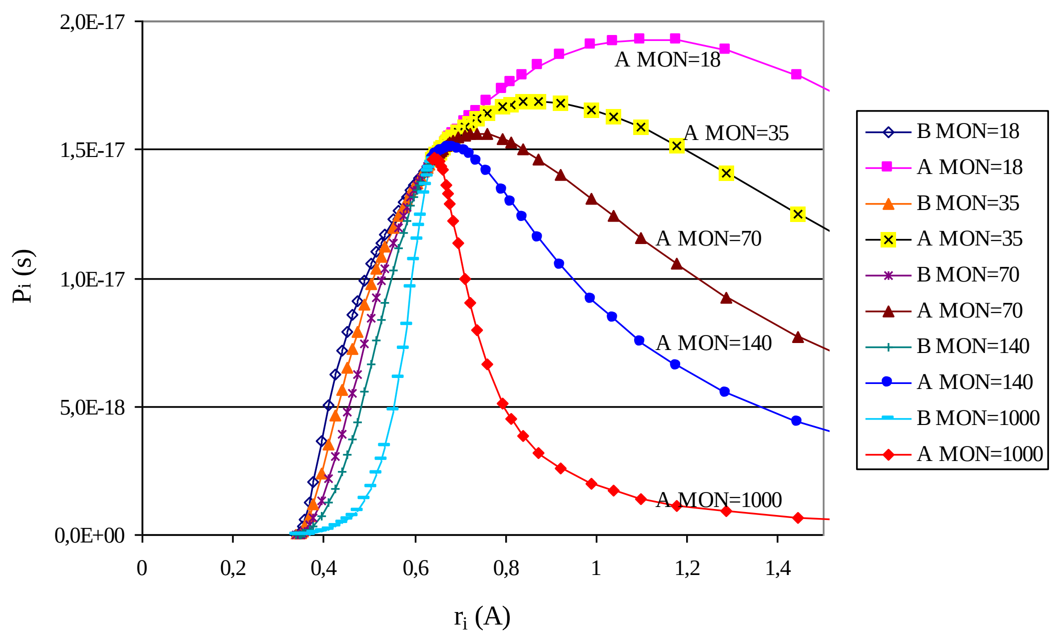

MON decrease causes displacements towards greater probabilities in any division because is in C_F numerator (2) or (3) and (9). In addition, P_i increase in any division provides that Maximum Probability is also displaced towards higher r_A (**Figure 8**). MON is only introduced by P26 [3], but its value is not established at this theory moment.

$$\downarrow MON \rightarrow \downarrow C_F \rightarrow \uparrow c_i \rightarrow \uparrow P_i$$

When MON is modified, Maximum Probability displacement has internal limit equal to $(r_i)_{d\rightarrow\infty}$ (11) [1] because:

- Maximum Probability is in EE_A.
- MON does not modify $(r_i)_{d\rightarrow\infty}$ since is not included in Victoria Equation.

$$(11)\ (r_A)_{d\rightarrow\infty} = (r_B)_{d\rightarrow\infty} = (r_i)_{d\rightarrow\infty} = \frac{-fz}{2(E_i)_{d\rightarrow\infty}} = \frac{-fz}{E_o} = \frac{-F}{E_o}$$

- This limit is achieved when MON→∞. P_i vs. r_i curve as MON increases (see curve with MON=1000) is transformed to that obtained with PEP=1 [3].

When MON decreases, Maximum Probability is in lower d_A if is taken into account:

- MON is not in Victoria Equation and therefore MON change does not modify relationship between division and r_i.
- Maximum Probability is displaced towards higher r_A that require lower d_A.

PEP explanation is similar to the view with MON since is also C_F (2) or (3) and does not affect Victoria Equation [1], but its effect is inverse. As with MON, PEP is in C_F numerator, but its preponderant effect is located in denominator ($d^{x\cdot PEP}$). PEP value is defined as 1 or 2 by P27 [3], but in Figure 9, PEP=3 and PEP=4 are shown by way of example.

$$\downarrow PEP \rightarrow \downarrow \text{Numerator and} \downarrow\downarrow \text{Denominator of } C_F \rightarrow \uparrow C_F \rightarrow \downarrow c_i \rightarrow \downarrow P_i$$

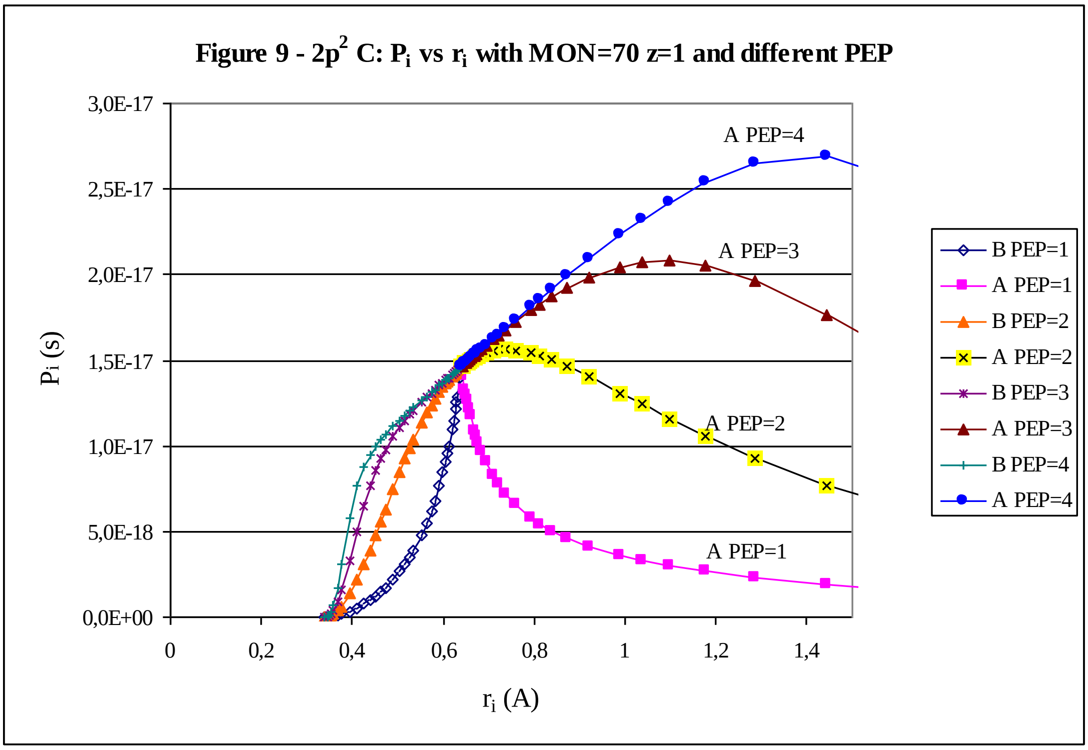

z Effective nuclear charge is in r_i Victoria Equation (11) and is also in $(r_i)_{d\to\infty}$ (12) and $(r_B)_{d\to 0}$ (13) [1]. F included in (11) is equal to fz (14) [1]. According to (11-13), z decrease causes curve overall displacement to r_i closer to nucleus. In contrast, z does not affect $(r_A)_{d\to 0}$ because is equal to infinite (Birth wavelength (λ) divided by d). These facts imply that z influence provoking displacement to r_i closer to nucleus is present for all division and only effect is fading when d→0. z value is marked by P14 [1], but only for external ns lobes. $2p^2$ C lobe is not included in P14 because is not ns and different z values (1.25 1 0.85 0.7 and 0.5) have been applied to see effect in **Figure 10**.

$$(11)\ r_A = \frac{-F - \frac{h\sqrt{-E_o}}{d m_e^{1/2}} - \sqrt{F^2 + \frac{h^2(-E_o)}{d^2 m_e}}}{2E_o}$$

$$(12)\ (r_A)_{d\to\infty} = (r_B)_{d\to\infty} = (r_i)_{d\to\infty} = \frac{-fz}{2(E_i)_{d\to\infty}} = \frac{-fz}{E_o} = \frac{-F}{E_o}$$

$$(13)\ (r_B)_{d\to 0} = \frac{-fz}{2E_o} = \frac{-F}{2E_o}$$

$$(14)\ F = \frac{Kq^2}{2} z = fz = 1{,}153538564 \bullet 10^{-28} z$$

$$(15)\ (r_A)_{d\to 0} = \frac{\frac{E_o\lambda}{d} - \sqrt{\frac{E_o^2\lambda^2}{d^2}}}{2E_o} = \frac{\frac{-2/E_o/\lambda}{d}}{2E_o} = \frac{\lambda}{d} = \infty$$

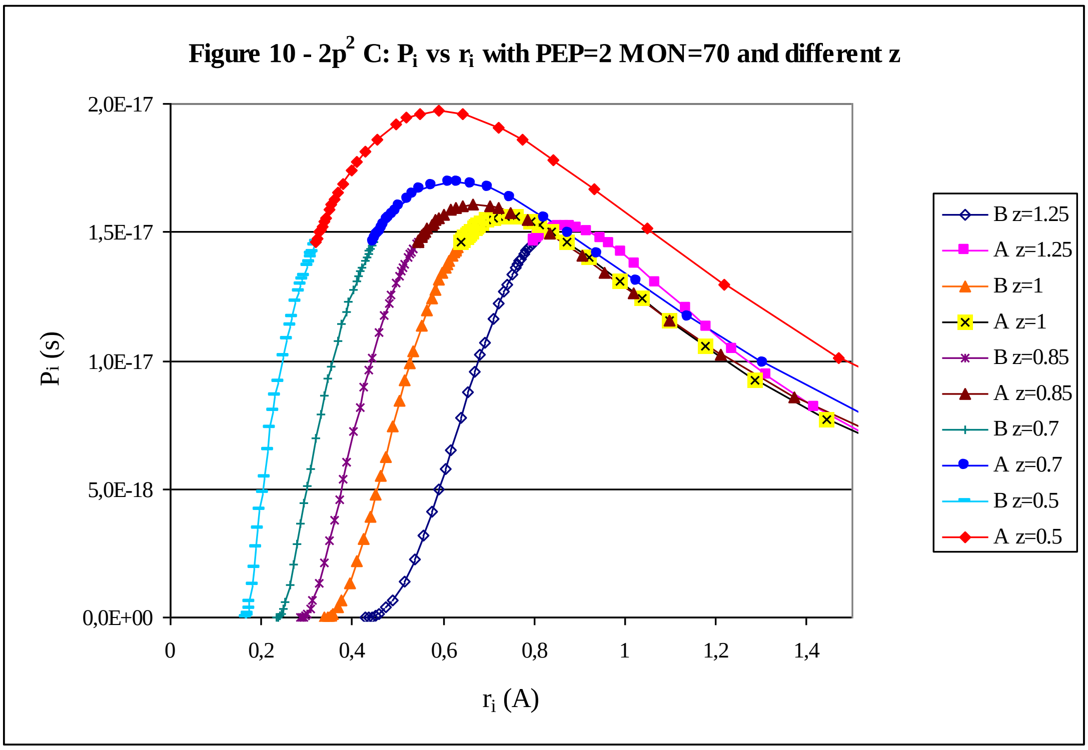

z variation effect is not as neat in P_i vs r_i curves as with MON (Figure 8) and PEP (Figure 9) and cross-curves are observed. This crossing is mainly due to curve displacement previously explained although there is also an effect on P_i (16) obtained in [3].

$$(16)\ P_i = \frac{\hbar}{C_F m_e v_i^2}$$

a) Direct action on v_i^2:

EE Kinetic Energy (Ek_i) and EE velocity (v_i) are related by (17) where $m_i = m_e/2$ [1] v_i^2 (18) is obtained from (17)

$$(17)\ Ek_i = \frac{1}{2} m_i v_i^2 = \frac{1}{4} m_e v_i^2$$

$$(18)\ v_i^2 = \frac{4Ek_i}{m_e}$$

Ek_i (19) is known by potential and kinetic energy relation of Bohr orbit balance applied to EE [1]. Also in [1], E_i is indicated (20) and Ek_i is reformulated (21) when (19) and (20) are considered.

$$(19)\ Ek_i = -\frac{EP_i}{2} = -E_i \quad \text{with } E_A + E_B = E_o$$

$$(20)\ E_i = -\frac{Kzq^2}{4r_i} = -\frac{fz}{2r_i}$$

$$(21)\ Ek_i = -E_i = \frac{fz}{2r_i}$$

Proportionality $P_i \ \alpha\ 1/v_i^2$ (16) is consistent with also being proportional to Ek_i inverse (17) and r_i/z (21) as summarized in (22):

$$(22)\ P_i \,\alpha\, \frac{1}{v_i^2} \,\alpha\, \frac{1}{Ek_i} = \frac{2r_i}{fz} \,\alpha\, \frac{r_i}{z}$$

Figure 11 shows behaviour of P_i with z=1/2 and z=1 (23), where (23) is probabilities ratio depending on z chosen.

$$(23)\ (P_i)_{ratio} = \frac{(P_i)_{z\,=\,1/2}}{(P_i)_{z\,=\,1}}$$

- P_i when z=1/2 is not twice that when z=1, although P_i is inversely proportional to z (22), because r_i must be taken into account.
- Separation between two P_i quotient curves complies that the one provides by two EE_A is above 1 and that provided by EE_B is below 1 because P_i is inversely proportional to Ek_i and energy balance (19) must be fulfilled [1].

- r_i is proportionate by r_i Victoria Equation and has points where this equation is simplified ($(r_B)_{d\to0}$ $(r_A)_{d\to0}$ y $(r_i)_{d\to\infty}$ are deduced in [1]) and whose solutions can be substituted in (22) to justify the trends in Figure 11:

  - $(P_B)_{d\to0}$ is proportional to $(-E_o)^{-1}$ and has no z influence (24), implying that probabilities quotient (23) tends to 1. Similarly, $(P_i)_{d\to\infty}$ is z independent (25) and its Pi ratio (23) is equal to 1.
  - Situation turns to z influence for the rest of situations, being emphasized when $(r_A)_{d\to0}$ (26). Starting from probabilities ratio (23) and $(P_A)_{d\to0}$ (26), probabilities ratio equal to ratio of its inverted z is obtained (27).

Figure 11 - Pi ratio (23) between z=1/2 and z=1

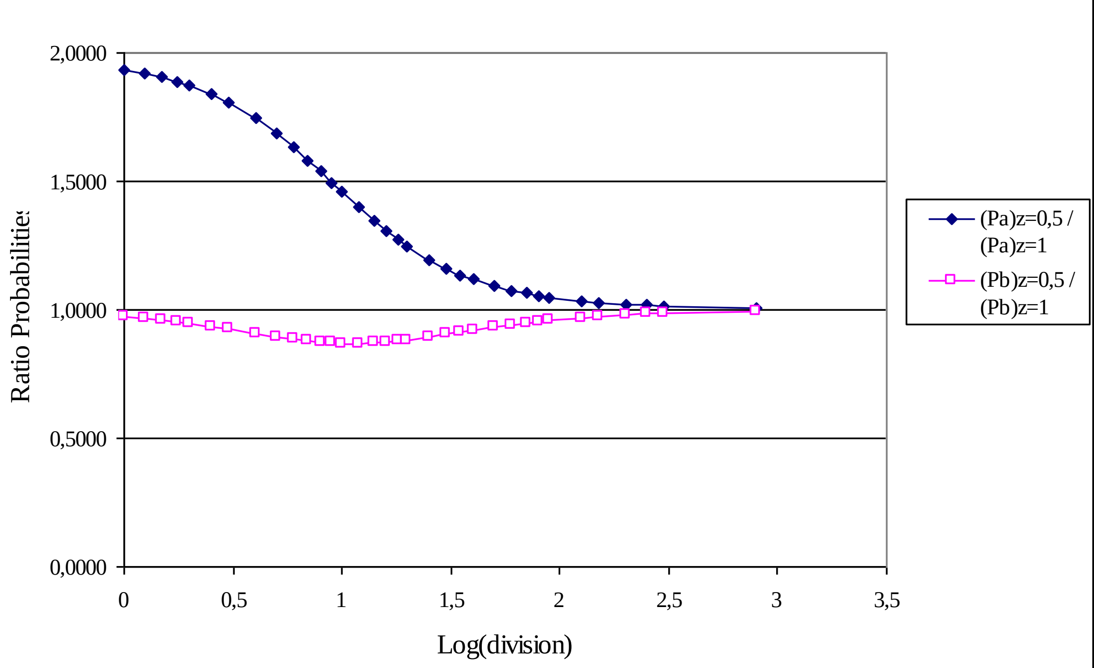

$$(24)\ (P_B)_{d\to0}\ \alpha\ \frac{2(r_B)_{d\to0}}{fz} = \frac{2}{fz}\frac{(-fz)}{2E_o} = -\frac{1}{E_o}$$

$$(25)\ (P_i)_{d\to\infty}\ \alpha\ \frac{2(r_i)_{d\to\infty}}{fz} = \frac{2}{fz}\frac{(-fz)}{E_o} = -\frac{2}{E_o}$$

$$(26)\ (P_A)_{d\to0}\ \alpha\ \frac{2(r_A)_{d\to0}}{fz} = \frac{2}{fz}\frac{\lambda}{d}\ \alpha\ \frac{1}{z}$$

$$(27)\ ((P_A)_{ratio})_{d\to0} = \frac{(P_i)_{z=1/2}}{(P_i)_{z=1}} = \frac{1}{1/2} = 2$$

b) Indirect role on C_F: Although z is not included in C_F, z affects division position (r_i) and d is critical in C_F.

Finally, after introducing J, MON, PEP, and z modification effect, a research line to be developed corresponds to C_F structure alteration. An example is change of x^2 (2) by x^3

(28) in numerator of different terms. In **Figure 12** is represented C_F with J=1 and J=10 and there are two possibilities with J=10 that are using (2) or (28). In Figure 12 nomenclature, "CF 10 Exp 3 A" is C_F with J=10 and x^3 (28) for A electronic extreme. Greater numerator implies acceleration towards higher compaction and therefore lower probabilities for the same d or r_i.

$$(28)\ C_{F-J\,order} = 2 + \sum_{x=1}^{J} \frac{x^3 * P * M}{d^{x*P}}$$

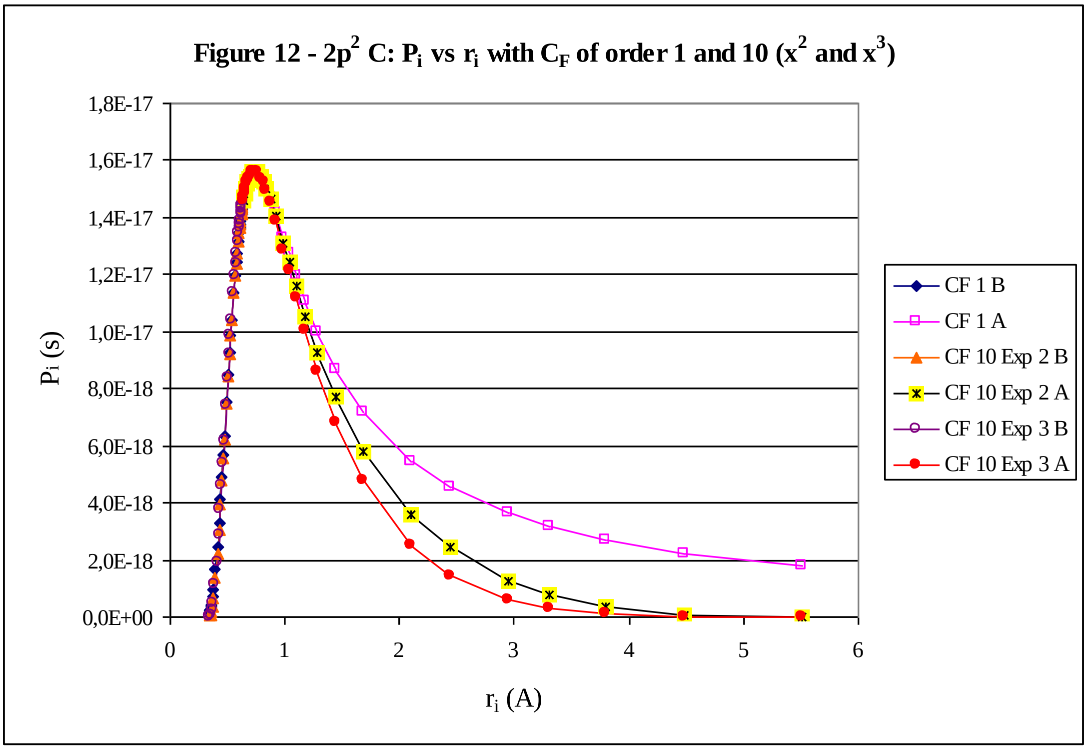

<u>Plane c_i-H_i Representation</u>

Orbital representation or H_i vs c_i representation (**Figure 13 and 14**) adds orbital closure to representation with first-order C_F [3]. Figure 13 is performed on 1:1 scale and orbital closure is only intuited and for this reason, in Figure 14, H_i is enlarged and c_i is reduced by to be able to clearly observe orbital enclosure. P_A existence up to $d \rightarrow 0$ (or $r_A \rightarrow \infty$) would imply that, by probabilities sum, P_A would be infinite when $r_A \rightarrow \infty$ and to avoid this, C_F with infinite J closes EE_A with d=1 and therefore also EE_B.

From now, CF to be used is (2) and J=10 is considered sufficient. (2) can be reformulated as (29) when PEP=P=2.

$$(29)\ C_{F-10\,order}(P=2) = 2 + \sum_{x=1}^{J} \frac{x^P * P * M}{d^{x*P}} = 2 + \sum_{x=1}^{J=10} \frac{2x^2 M}{d^{2x}}$$

Following steps are going to be:

a) Shape and filling of orbital
b) Electronic coupling development (initiated in [3]) and that is NIN concept part. As indicated in [3], this extension is pending Probability concept conclusion that has been advanced in [3] and this article. Final step related to a) point is necessary to strengthen Probability concept and be able to continue with Electronic coupling.

Figure 13 - 2p^2 C: Orbital representation with C_F order 1 and 10: x^2 and x^3

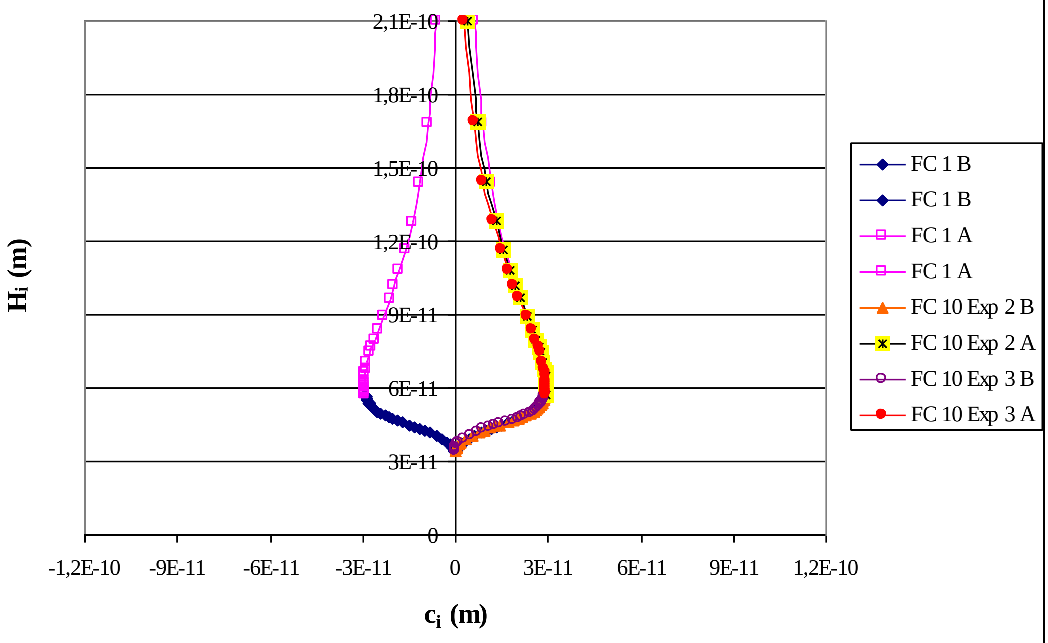

Figure 14 - Figure 13 orbital representation with orbital closure detail

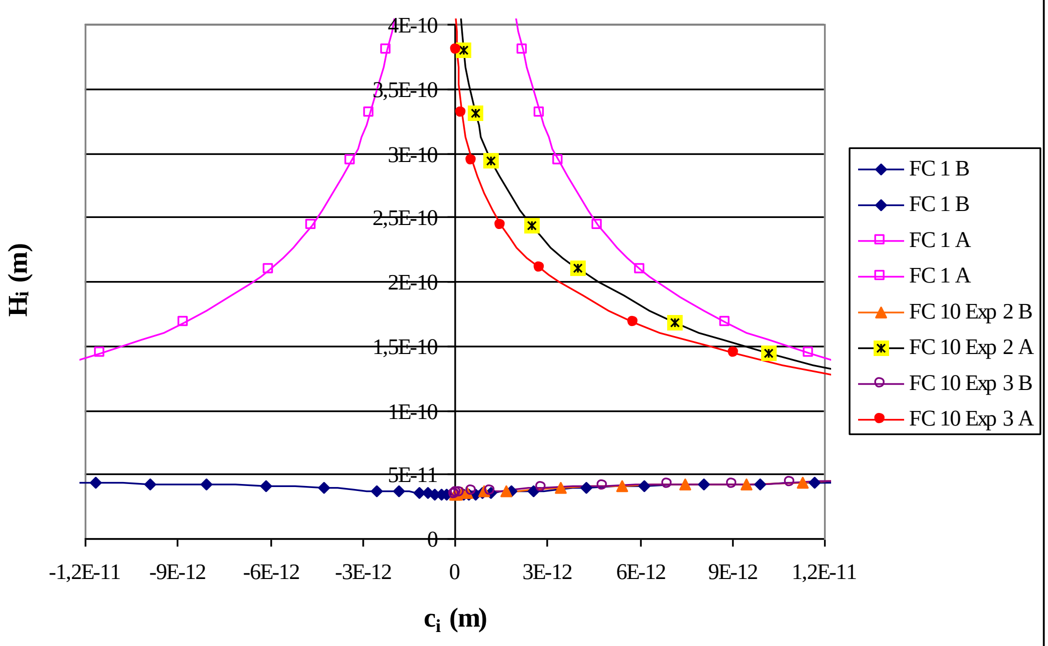

BIBLIOGRAPHY

[1] Javier Silvestre. Victoria Equation - The dark side of the electron. (Document sent to vixra.org)
[2] Javier Silvestre. Electronic extremes: orbital and spin (introduction). (Document sent to vixra.org)
[3] Javier Silvestre. Relations between electronic extremes: Rotation time as probability and first Feliz solution. (Document sent to vixra.org)
[4] Kramida, A., Ralchenko, Yu., Reader, J., and NIST ASD Team (2014). NIST Atomic Spectra Database (ver. 5.2), [Online]. Available: http://physics.nist.gov/asd
[5] S. Fraga, J. Karwowski, K. M. S. Saxena, Handbook of Atomic Data, Elsevier, Amsterdam, 1979.
[6] Desclaux JP. Relativistic Dirac-Fock expectation values for atoms with Z = 1 to Z = 120. Atom Data Nucl Data Tables 1973;12: 311-406.

Abbreviations List

Suffix indicates electronic extreme considered and i suffix is used to both electronic extremes (EE_i). Following Table indicates abbreviations used in this theory and its use in article in question is marked with X. 4 is present article

Abbreviations Table						
Abbreviation	**1**	**2**	**3**	**4**	**5**	**Meaning**
α_{NOA}					X	Nucleus-Orbit-Angle
a_o			X			Bohr radius
AL					X	Angular Limit
c_i		X	X	X	X	EE Orbital circumference
C_F		X	X	X	X	Wavelength compaction factor
C_{MON}					X	C_F without C_{POTI}
C_{POTI}					X	Probabilistic Orbital Tide in Third Feliz Solution
$C_{POTI\text{-}AL}$					X	C_{POTI} Angular Limit
$C_{POTI\text{-}GAL}$					X	C_{POTI} Geometric Angular Limit
$C_{POTI\text{-}LAG}$						C_{POTI} Lobe Always growing
d	X	X	X	X	X	Birth wavelength division or simply, division
EE	X	X	X	X	X	Electronic extreme
E_o	X	X	X	X	X	Initial, birth or output energy
E_i	X		X	X		EE energy
Ek_i	X		X	X		EE kinetic energy
EP_i	X			X		EE potential energy
ES	X	X				Equi-energetic state
f	X		X	X	X	Constant in Victoria Equation
F	X		X	X	X	Constant f multiplied by z
GAL					X	Geometric Angular Limit

h	X	X	X		X	Planck´s constant
ħ		X		X	X	Reduced Planck´s constant
h_i	X		X			Planck´s constant adapted to EE
H_i		X	X	X	X	EE Circular orbit height
IE	X	X		X	X	Ionization Energy
m_e	X	X	X	X	X	Electron mass
m_i	X		X	X		EE mass
J				X	X	C_F order in Second Feliz Solution (From x=1 to J)
K_P			X			Probability constant in Variable C_F
λ_{Birth} λ	X	X		X	X	Birth wavelength
λ_c	X					Electron classic wavelength
λ_i	X	X	X	X		EE wavelength
$\lambda_{i\text{-}Birth}$	X					EE wavelength when $d \rightarrow \infty$
LAG					X	Lobe always growing
M			X	X	X	MON (Modified Orbital Number)
MON			X	X	X	Modified Orbital Number
NIN	X		X	X		Negative in Negative (Electron in electron concept)
OAM		X				Orbital Angular Momentum
OPA		X				Orbital Planes Axis
P_i			X	X	X	EE Probability
P			X	X	X	PEP (Principal Electronic Part)
PEP			X	X	X	Principal Electronic Part
q_e	X					Electron charge
q_i	X					EE charge
q_{ip}	X					Proton charge
r_{AB}	X					Difference in nucleus distance between EE_A and EE_B
r_O	X					Nucleus distance when EE_i is in pivot or initial position
r_i	X	X	X	X	X	Distance between nucleus and EE
SAM		X				Spin Angular Momentum
SMM		X				Spin Magnetic Momentum
SSM	X		X			Secondary Swinging Movement
v_i	X	X	X	X	X	EE velocity
z	X	X	X	X	X	Effective nuclear charge
Z	X					Atomic number

ARTICLES INDEX		
Part	**Number**	**Title**
Part I - Victoria Equation and Feliz Solutions	01	Victoria Equation - The dark side of the electron.
	02	Electronic extremes: orbital and spin (introduction)
	03	Relations between electronic extremes: Rotation time as probability and Feliz I.
	04	Feliz II the prudent: Probability radial closure with high order variable C_F
	05	Feliz III The King Major: Orbital filled keeping Probability electronic distribution.
	06	Feliz IV Planet Coupling: Probability curves NIN coupling from origin electron.
	07	NIN Coupling values in n=2 and Oxygen electronic density.
	08	Electron Probability with NIN coupling in n=2.
	09	Electron probability with NIN coupling in n>2 and necessary NIN relationships.
Part II – Excited electron: Tete Vic and LAN	10	Excited electrons by Torrebotana Central Line: Tete Vic Equation.
	11	Excited electrons: LAN plains for Tete Vic Equation.
	12	Relation of Riquelme de Gozy: LAN linearity with energy of excited states.
	13	Relation of Fly Piep de Garberí: LAN^{-1} and Ionization Energy.
	14	Relation of Silva de Peral & Alameda: LAN interatomicity with energetic relation.
	15	Relation of Silva de Peral & Alameda II: jump from n_ss to ns.
	16	SPA III: Mc Flui transform for Silpovgar III and Silpovgar IV.
	17	SPA IV: Silpovgar IV with Piepflui. Excess Relativistic: influence in LAN and SPA
	18	Feliz Theory of Eo vision - Relativistic II: influence in Riquelme de Gozy
	19	Pepliz LAN Empire I: $LAN_{n\to\infty}$ vs. LAN(P50)
	20	Pepliz LAN Empire II: $LAN_{n\to\infty}$ vs. LAN(P50)
Part III - NIN: C_{PEP} & C_{POTI}	21	Electron Probability: PUB C_{PEP} I (Probability Union Between C_{PEP}) - Necessary NIN relationships
	22	Electron Probability: PUB C_{PEP} II in "Flui BAR" (Flui (BES A (Global Advance) Region)
	23	Orbital capacity by advancement of numbers - Electron Probability: PUB C_{PEP} III: "Flui BAR" II and C_{PEP-i}
	24	Electron Probability: 1s electron birth: The last diligence to Poti Rock & Snow Hill Victoria
24 hours of new day		